Electronic Supplementary Material (ESI) for Polymer Chemistry.

Supporting Information

Polypropylene-based transesterification covalent adaptable networks with internal catalysis

Yuanchu Gao, Hui Niu*

State Key Laboratory of Fine Chemicals, School of Chemical Engineering, Dalian University of Technology, Dalian 116024, China

1 Small Molecule Model Study

Synthesis of 1-decyl butanedioate (**1a**) [1]

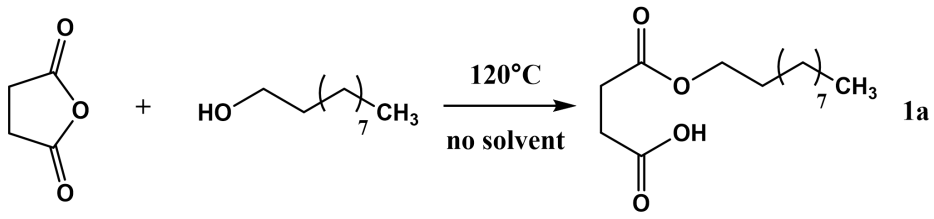

Scheme S1 Synthesis of 1-decyl butanedioate (**1a**)

Succinic anhydride (6.00 g, 59.98 mmol, 1.00 eq.) dissolved in 1-decanol (10.44 g, 65.98 mmol, 1.10 eq) was heated to 120 ℃ for 4 h. After reaction, the solution was cooled to room temperature and slowly poured into hexane (100 mL). The mixture was then placed in an ice bath for 1 h. The resulting solid was filtered under reduced pressure and washed with cold hexane (60 mL) to yield **1a** as white needles (7.75 g, 50%).

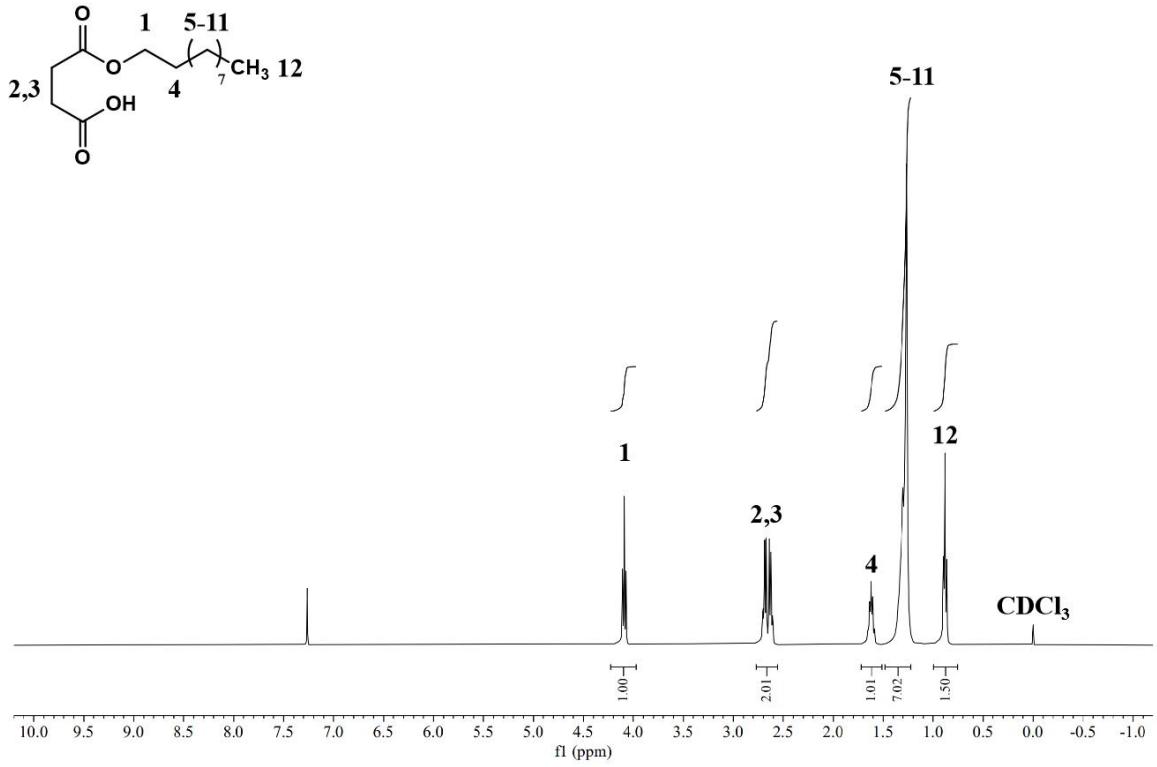

Figure S1 ^{1}H-NMR spectrum of **1a**

Synthesis of 1-(2-phenylethyl) butanedioate (**1b**) [2]

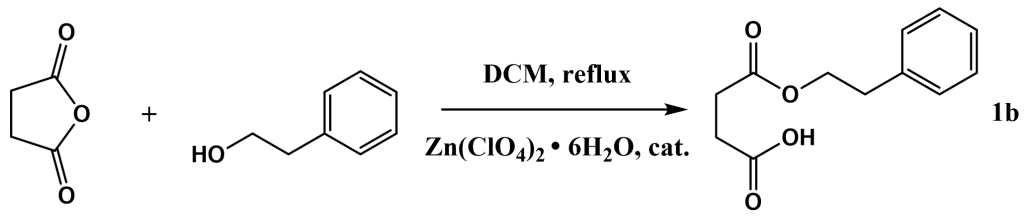

Scheme S2 Synthesis of 1-(2-phenylethyl) butanedioate (**1b**)

Succinic anhydride (3.44 g, 34.38 mmol, 1.05 eq.), 2-phenylethanol (2.00 g, 32.74 mmol, 1.00 eq.), $Zn(ClO_4)\cdot 6H_2O$ (catalytic) and DCM were added to a flask. The mixture was heated to reflux for 1 h. After cooled to room temperature, the mixture was washed with saturated $NaHCO_3$ solution. The aqueous layer was separated and extracted with DCM. The combined organic layer was dried with $MgSO_4$ and and concentrated to yield **1b** as white crystals (2.83 g, 39%).

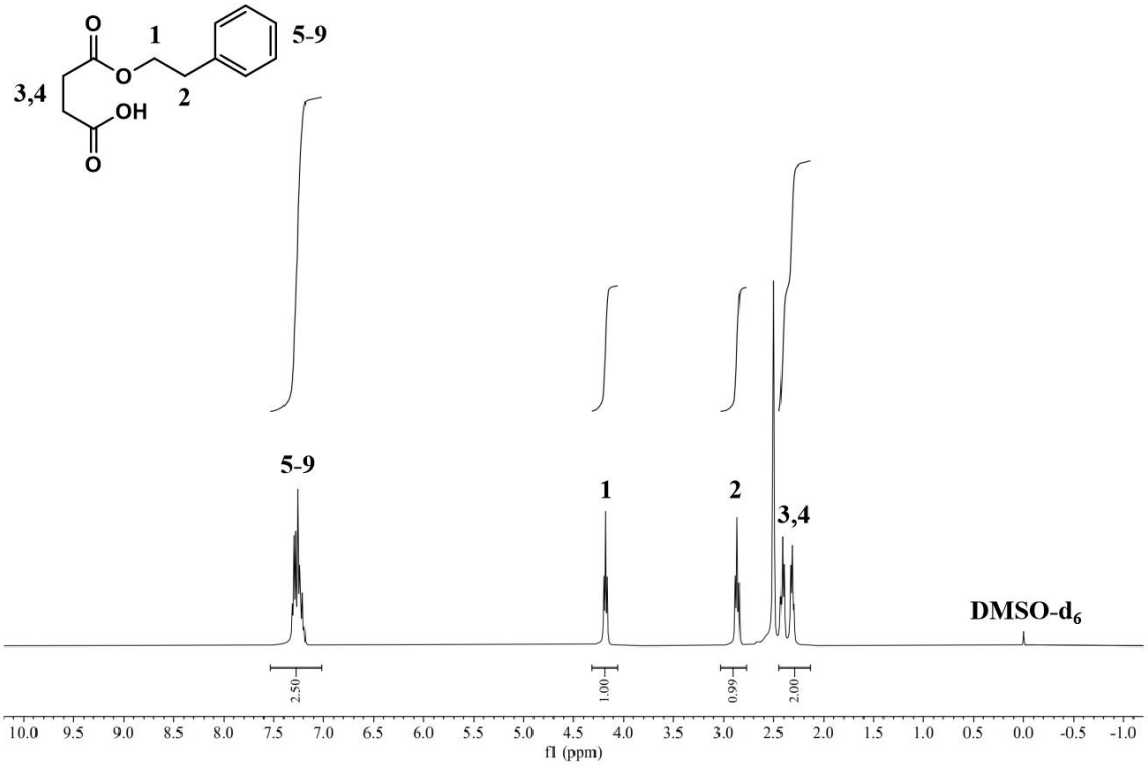

Figure S2 ^{1}H-NMR spectrum of **1b**

Synthesis of decyl butanoate (**2a**) and 2-phenylethyl butanoate (**2b**) [3]

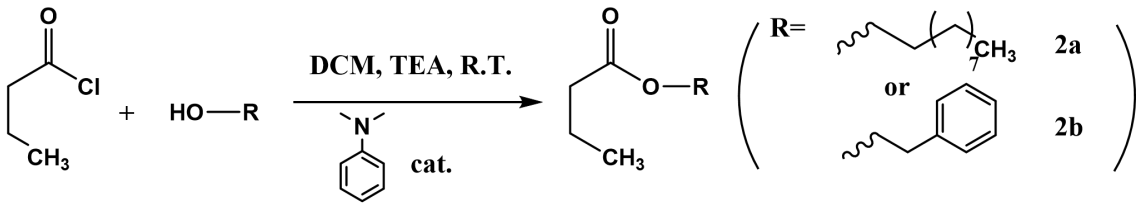

Scheme S3 Synthesis of decyl butanoate (**2a**) and 2-phenylethyl butanoate (**2b**)

The preparation of **2a** and **2b** followed similar steps. 1-decanol (3.00 g, 18.95 mmol, 1.00 eq.) for synthesizing **2a** or 2-phenylethanol (2.00 g, 16.37 mmol, 1.00 eq) for **2b**, TEA (1.10 eq.), DMAP(catalytic) were dissolved in 30 mL of DCM in a flask. Butyryl chloride (1.10 eq) dissolved in DCM (10 mL) was added dropwise to the flask with an ice water bath. The reaction was allowed to warm up to room temperature and stirred overnight. After reaction, the mixture was filtered under reduced pressure. The resulting oil was washed with saturated $NaHCO_3$ solution and brine. Then the organic layer was dried with $MgSO_4$, filtered and concentrated to yield **2a** as colorless oil(2.81 g, 65%) or **2b** as yellowish oil(2.14 g, 68%).

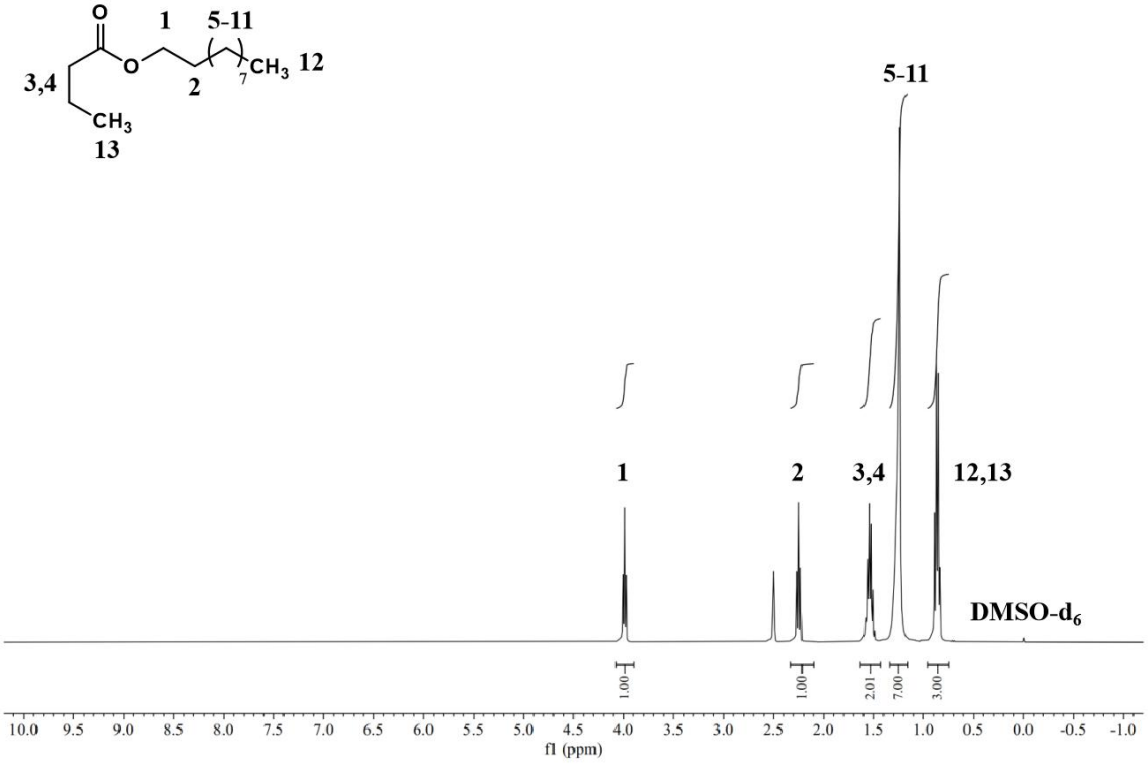

Figure S3 ^{1}H-NMR spectrum of **2a**

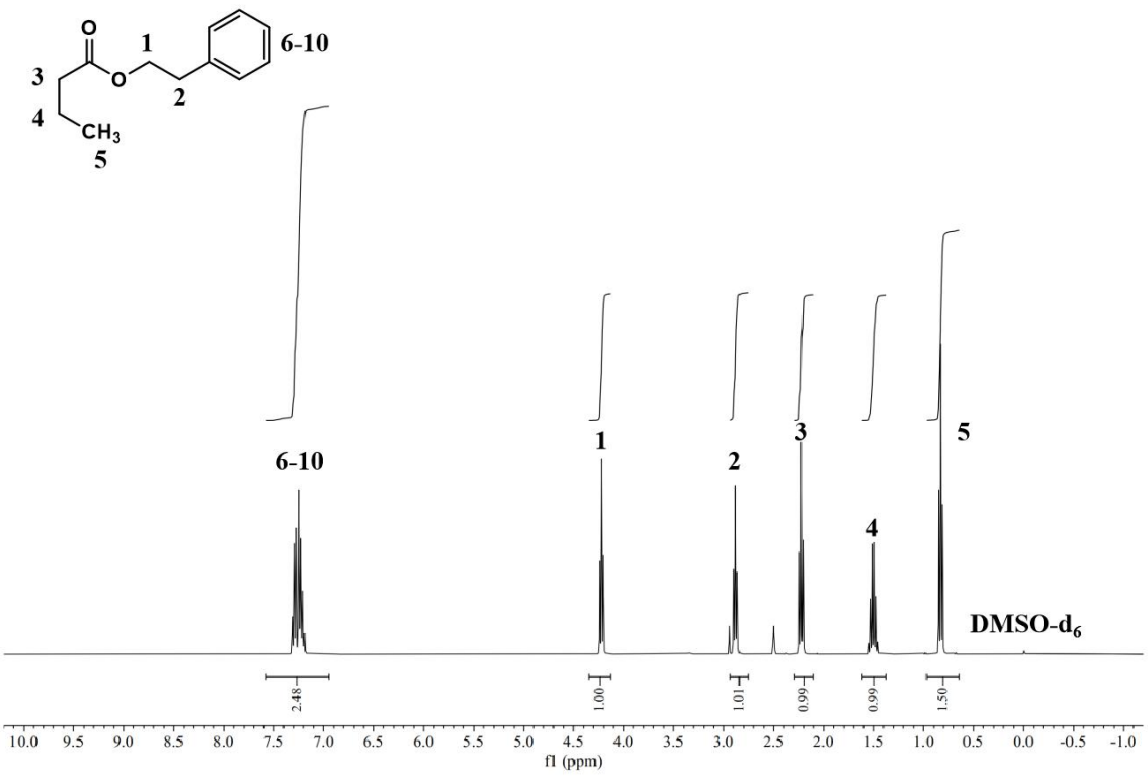

Figure S4 ^{1}H-NMR spectrum of **2b**

Quantitative calculations of exchange kinetics

The quantitative calculations of exchange kinetics are based on the ^{1}H-NMR spectra of two model reactions at designed temperatures for different reaction times. We use the percentage of the starting ester remaining (R) to measure the progress of reactions. Taking the reaction between **1a** and 2-phenylethanol at 120 ℃ (**Fig. 1B**) and the reaction between **2a** and 2-phenylethanol at 160 ℃ (**Fig. S5**) as examples, the formulas are as follows:

$$R_{1a} = (1 - \frac{A_{4.22}/2}{A_{0.86}/3}) \times 100\% \quad \text{(S1)}$$

$$R_{2a} = (1 - \frac{A_{4.22}/2}{A_{0.86}/6}) \times 100\% \quad \text{(S2)}$$

where A_x represent integral areas of peaks at given chemical shifts. The -CH_3 hydrogens are chosen as the reference since their chemical shifts are almost unaffected before or after reactions.

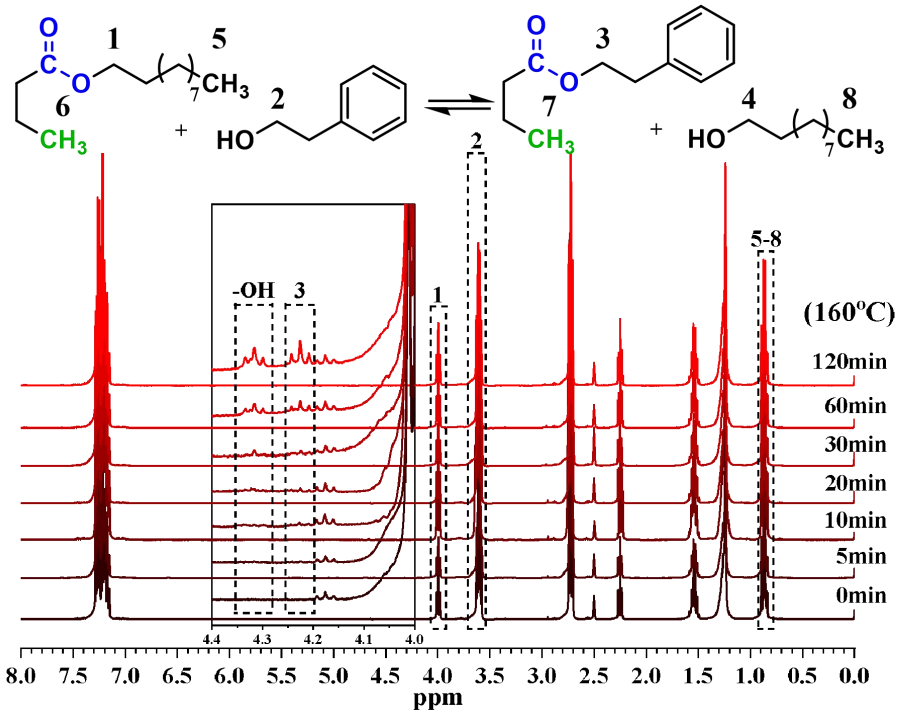

Fig. S5 ^{1}H-NMR spectra of the reaction between **2a** and 2-phenylethanol at 160 ℃ for different reaction times

Kinetics approximation of model reactions

Referring to the work of Du Prez et al., the kinetics of the model reactions are approximated by the pseudo-first order method with the following formula[4]:

$$R_{1a} \text{ or } R_{2a} = [1 - x_\infty + x_\infty \exp(\frac{-kt}{x_\infty})] \times 100\% \quad \text{(S3)}$$

where t is the reaction time and x_∞ is an estimated parameter according to the reference[5]. After acquiring the approximation of rate constant (k), the Arrhenius plot can be obtained according to the equation below:

$$\ln(k) = \ln(A) - \frac{E_a}{RT} \quad \text{(S4)}$$

where A is the pre-exponential factor and an apparent activation energy (E_a) can be given.

The kinetic approximations reveal that the reaction rate of the succinic monoester is slower than that of the phthalic monoester reported under the same conditions. Take different k at 140 °C as examples. The k of succinic monoester (0.01175 s^{-1}) is about one third of the k of succinic monoester (0.0388 s^{-1})[4], indicating the weakening of NGP due to lack of conjugation structures.

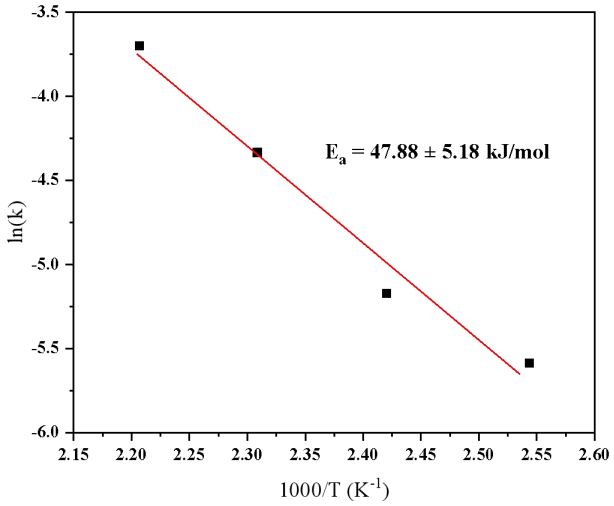

Fig. S6 Arrhenius plot of **1a** and 2-phenylethanol exchange kinetics

2 Material Synthesis

Calculation of anhydride grafting yields of PP-SA (y)

Based on the results of acid-base titration, the anhydride grafting yield of PP-SA (y) can be calculated according to the following formula:

$$y\ (\text{mol / g}) = \frac{C_1 \times (V_1 - V_b) - C_2 \times V_2}{2 \times m} \quad \text{(S5)}$$

where V_1, C_1, V_2, C_2 are the volume and concentration of KOH-EtOH or HCl-EtOH solution used in titration, respectively. V_b is the volume of KOH-EtOH solution consumed by the blank sample and m is the mass of PP-SA used during titration.

Detailed information of PP-SA materials

Table S1 Detailed information of PP-SA materials

Materials	χ_c (%)	$T_{d,5\%}$ (℃)	MFR (g/10min)	y^a (10^{-4}·mol/g PP)	M_n (10^4)	$y_a{}^e$
Commercial PP	48.7%	416.0	1.9±0.2	-	3.60	-
PP-SA-1	33.5%	426.5	0.9±0.1	0.180±0.040[b]	3.39	0.61±0.14
				0.136±0.018[c]		0.46±0.06
PP-SA-2	47.3%	405.9	3.1±0.2	1.157±0.042[b]	3.61	4.18±0.15
				0.760±0.026[c]		2.74±0.09
				0.831±0.047[d]		3.00±0.17
PP-SA-3	48.4%	407.8	54.5±0.9	0.832±0.020[b]	2.80	2.33±0.06
				0.289±0.035[c]		0.81±0.10
PP-SA-4	41.3%	412.6	77.4±2.3	0.885±0.029[b]	2.68	2.37±0.08
				0.575±0.010[c]		1.54±0.03

[a] Anhydride grafting yield of PP-SA.

[b] Samples determined by titration before acetone extraction.

[c] Samples determined by titration after acetone extraction.

[d] Samples determined by titration after 110 ℃ vacuum heating for 24 h.

[e] Average number of anhydride grafts per PP chain.

The results in **Table S1** were obtained from the data shown in **Fig. S7-S9**.

The value y_a represents average number of anhydride grafts per PP chain of PP-SA samples, which can be estimated according to the following formula:

$$y_a = y \times M_n \times 1\ \text{g/mol} \quad \text{(S6)}$$

where y is the anhydride grafting yield of PP-SA, and M_n is the number-average molecular weight of PP-SA samples.

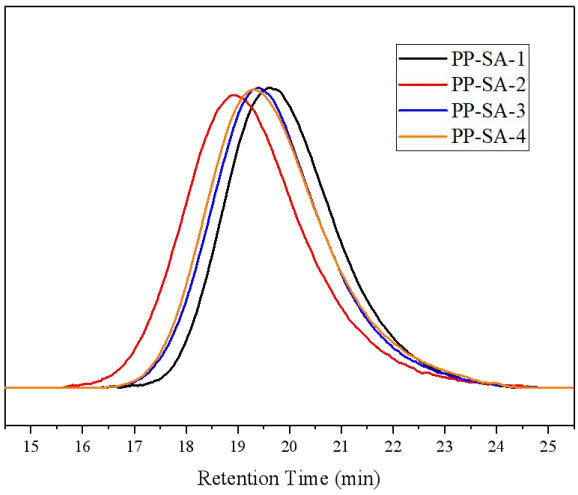

Figure S7 GPC spectra of PP-SA

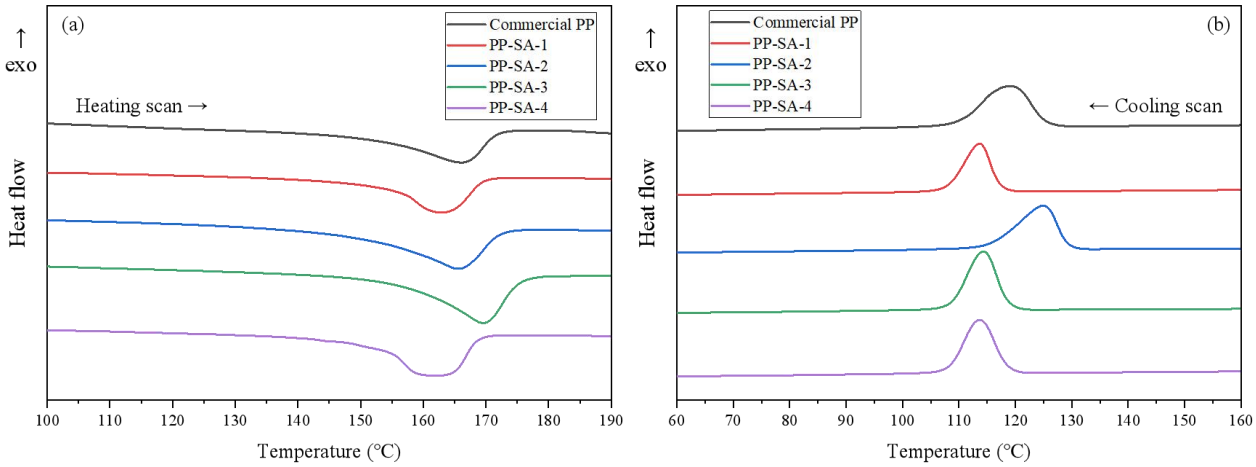

Figure S8 DSC thermogram of different PP/PP-SA
(a) 2nd heating scan of melting endotherm (b) cooling scan of crystallization exotherm

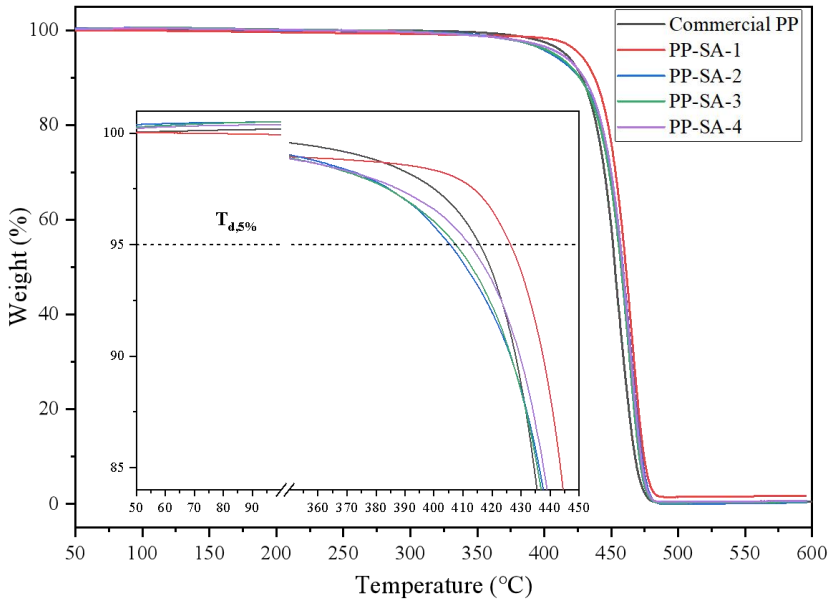

Figure S9 TGA spectra of different PP/PP-SA in nitrogen

Discussion of the characterization results of PP-SA materials

For the construction of PP-CANs, four grades of PP-SA were obtained and characterized in detail (**Table S1**). All PP-SA were subjected to acid-base titration to investigate their SA grafting yield (*y*), and their FTIR spectra were obtained. To exclude the disturbance of unreacted anhydrides on *y*, these PP-SA extracted with acetone were similarly assayed. The peaks at 1830 and 1780 cm^{-1} in FTIR spectra are attributed to asymmetric and symmetric stretching vibrations of the carbonyl groups in the anhydride, respectively (**Fig. S10**). The stretching vibrations of the ketone structures formed by side reactions of PP in radical grafting[6] and the carbonyl groups formed by partially hydrolyzed anhydrides together contribute to the peaks at 1730 cm^{-1}, so they do not disappear even after strict heat treatments for dehydration.

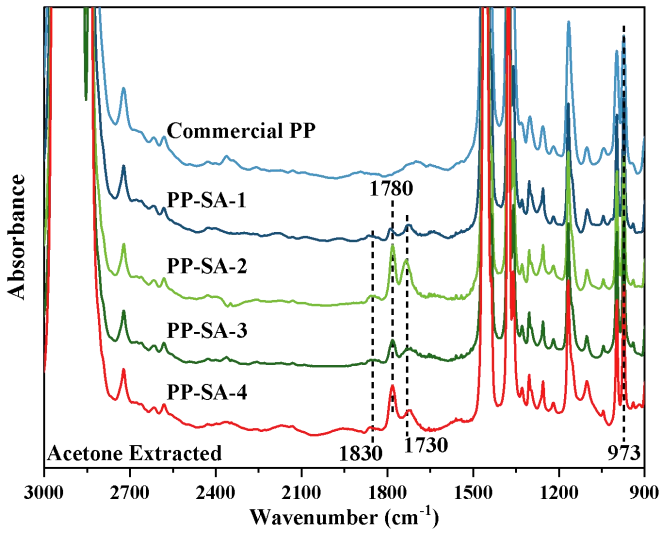

Fig. S10 FTIR spectra of commercial PP in hand and four grades of PP-SA extracted by acetone

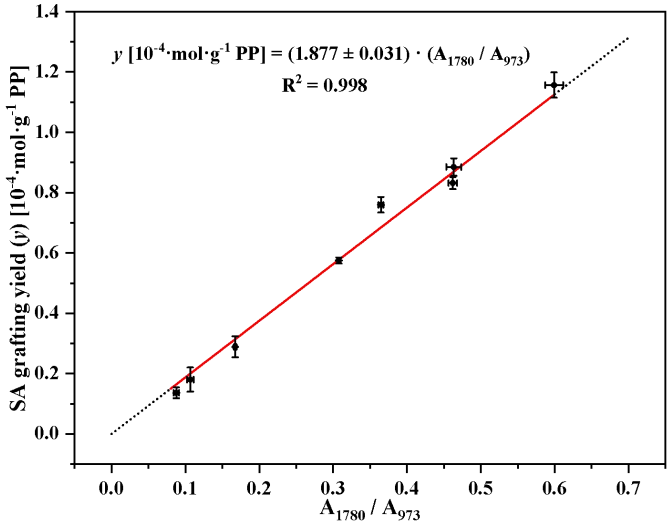

Fig. S11 Graph of *y* against the ratio of the characteristic absorbance of anhydrides at 1780 cm^{-1} to the absorbance of the internal standard at 973 cm^{-1}

Because of the complex structural information contained in peaks at 1730 cm^{-1}, we picked peaks at 1780 cm^{-1}, which only represent the anhydride amount of the system, for subsequent characterization. According to Beer-Lambert law, a close linear correlation is established by plotting the ratio of the absorbance at 1780 cm^{-1} to the absorbance of the internal standard at 973 cm^{-1} against the results of y (obtained through acid-base titration results of all samples before and after extraction) in **Fig. S11**. This provides a basis for quantitative characterizations of the residual anhydride amount after reactive processing.

Combining the number-average molecular weight (M_n) of PP-SA, we can further gain the average number of anhydride grafts per PP chain (y_a). Limited by the ceiling temperature of polymerization, MA is substantially unable to homopolymerize at PP reactive processing[7], which is advantageous for the construction of PP-CANs since potential crosslinking sites are not wasted by overlap due to homopolymerization. However, we would still like to use samples with relatively higher y_a values to achieve more pronounced networks. Based on this judgment as well as the *MFR* and thermal properties, we chose PP-SA-2, which is most similar to the commercial PP in hand, for PP-CANs fabrication. Considering that extraction is not suitable for bulk sample treatment, PP-SA-2 were placed under vacuum at 110 ℃ for 24 h before use to remove the residual unreacted MA[8]. Both titration and FTIR results show that most unreacted anhydrides can be successfully eliminated.

3 Material characterization and properties

Inference of the proportion of reacted anhydride

Due to the close linear correlation obtained in **Fig. 2B**, the reductions of SA exhibited in FTIR spectra allow quantitative inference of the esterification progress (the proportion of reacted anhydride, *P*) as in the following formula:

$$P(\%) = \frac{(A_{1780} / A_{973})_{\text{PP-SA}} - (A_{1780} / A_{973})_x}{(A_{1780} / A_{973})_{\text{PP-SA}}} \times 100\% \qquad \text{(S7)}$$

where $(A_{1780}/A_{973})_{\text{PP-SA}}$ represents the ratio of the absorbance at 1780 cm^{-1} to the absorbance at 973 cm^{-1} of PP-SA, and $(A_{1780}/A_{973})_x$ represents the ratio of the absorbance at 1780 cm^{-1} to the absorbance at 973 cm^{-1} of PP-CANs or comparison samples. Absorbances at 1730 cm^{-1} is unsuitable for this calculation since they include the contribution of ketone groups due to the side reactions between PP chains and radicals.

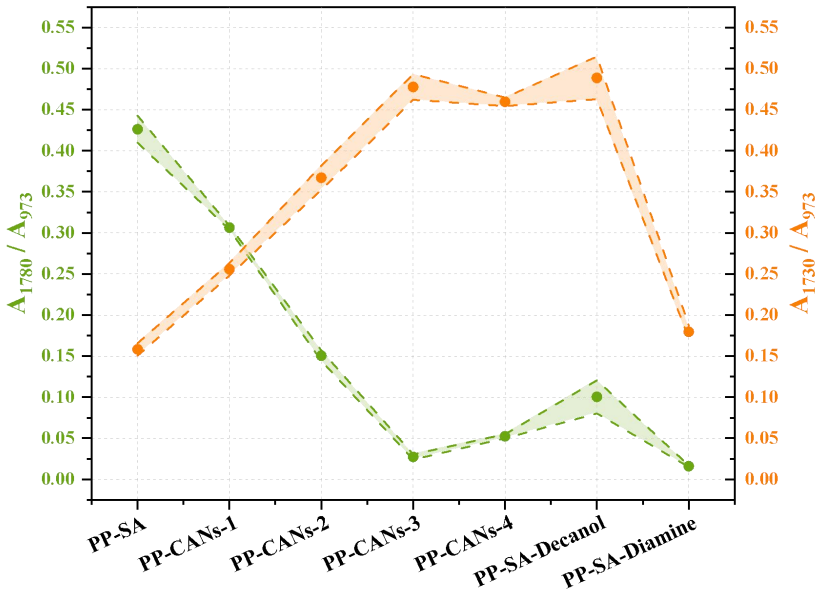

Fig. S12 Ratio of the absorbance at 1780 cm^{-1} (or 1730 cm^{-1}) to the absorbance at 973 cm^{-1} of PP-CANs and comparison samples

Thermal property data of PP-CANs and comparison samples

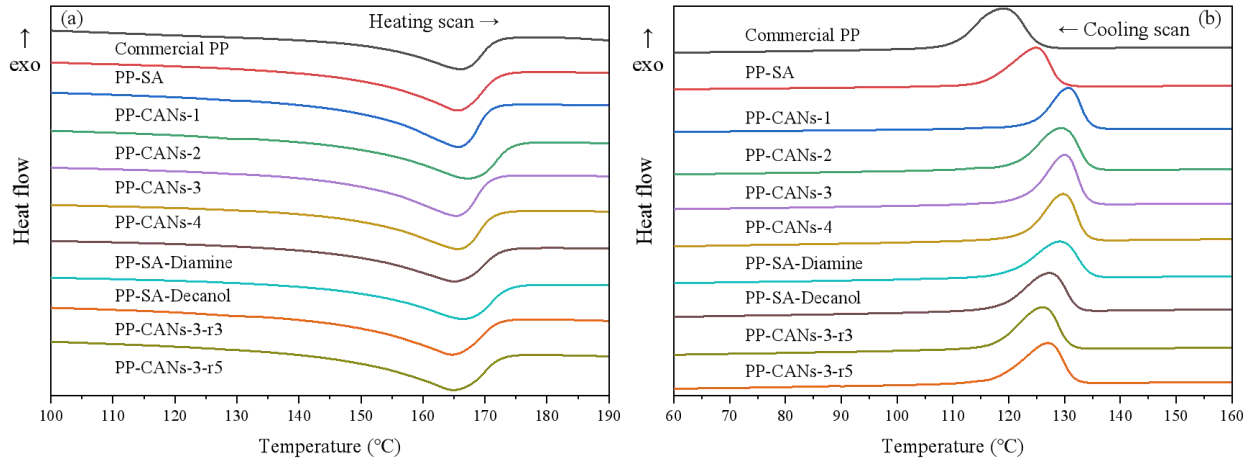

Figure S13 DSC thermogram of PP-CANs and comparison samples
(a) 2nd heating scan of melting endotherm (b) cooling scan of crystallization exotherm

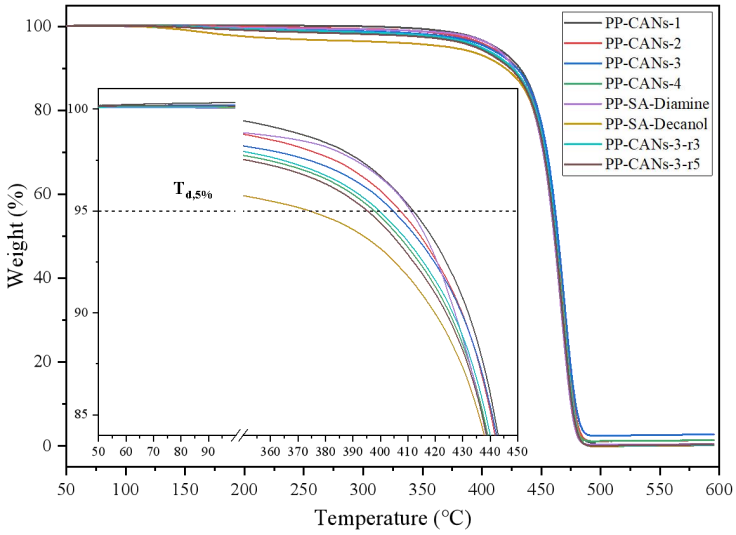

Figure S14 TGA spectra of PP-CANs and comparison samples acquired in N_2 atmosphere

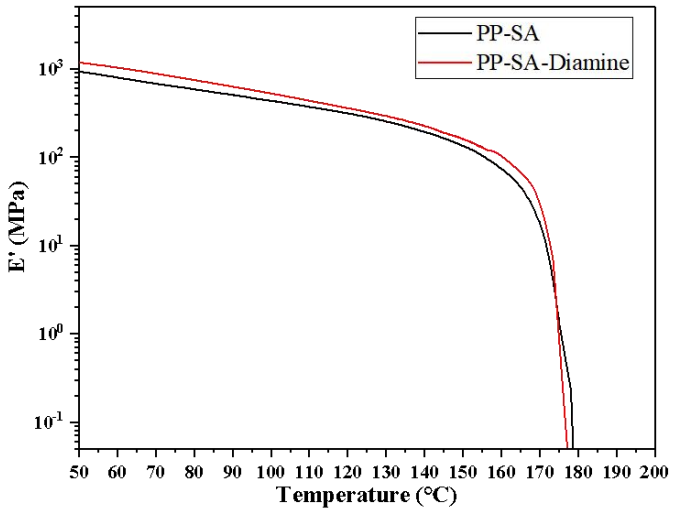

Figure S15 DMA spectra of PP-SA and PP-SA-Diamine

Stress relaxation data of PP-CANs and comparison samples

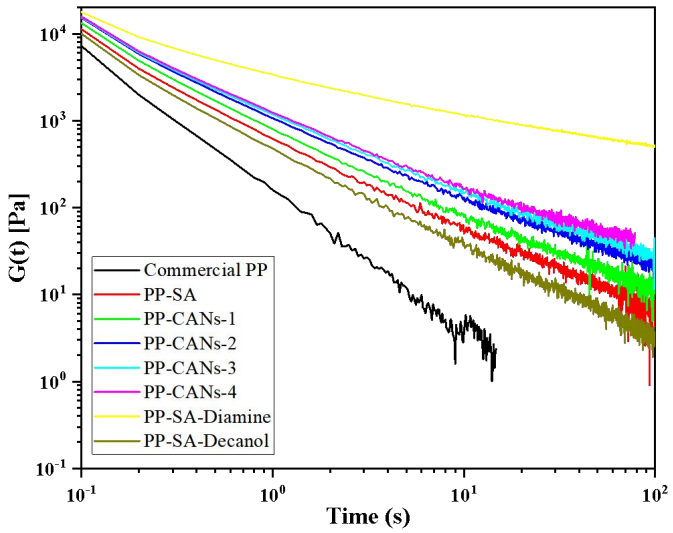

Fig. S16 Original stress relaxation curves of PP-CANs and comparison samples

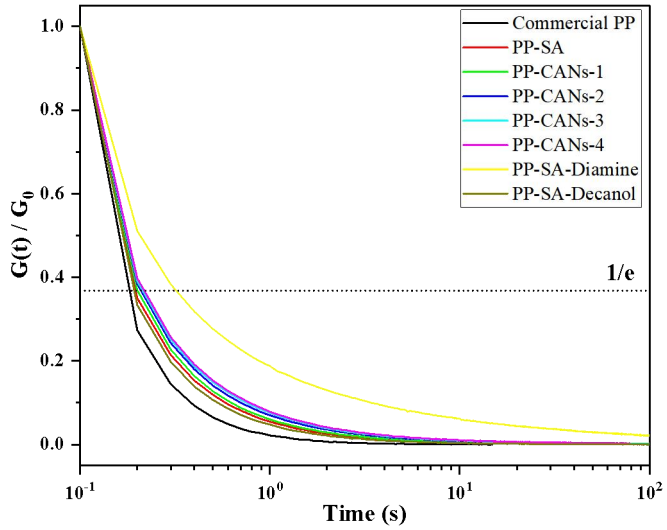

Fig. S17 Normalized stress relaxation curves of PP-CANs and comparison samples

Mechanical property data of PP-CANs and comparison samples

Table S2 Tensile properties of PP-CANs and comparison samples

Samples	Young's Modulus (E) [MPa]	Elongation at Break (ε) [%]	Yield stress (σ_y) [MPa]
Commercial PP	700.9±10.8	504.1±36.5	34.91±1.20
PP-SA	746.8±22.1	530.2±44.4	33.80±0.18
PP-CANs-1	721.5±10.1	491.3±60.8	42.78±0.48
PP-CANs-2	764.9±30.9	494.4±52.6	39.01±0.58
PP-CANs-3	836.1±31.2	447.8±74.1	38.03±0.74
PP-CANs-4	723.1±22.1	469.8±46.8	37.07±0.19
PP-SA-Diamine	889.3±52.3	164.5±94.3	36.51±1.19
PP-SA-Decanol	660.0±24.9	604.9±10.6	36.72±2.13
PP-CANs-3-r3[a]	828.0±31.2	351.2±14.4	38.18±0.18
PP-CANs-3-r5[b]	828.7±22.6	357.5±15.1	37.41±1.00

[a] PP-CANs-3 sample after 3 crushing and remodeling cycles.

[b] PP-CANs-3 sample after 5 crushing and remodeling cycles.

Young's Modulus, elongation at break and yield stress results of PP-CANs and comparison samples in **Table S2** were obtained from the data presented in **Fig. S18** and **S20**.

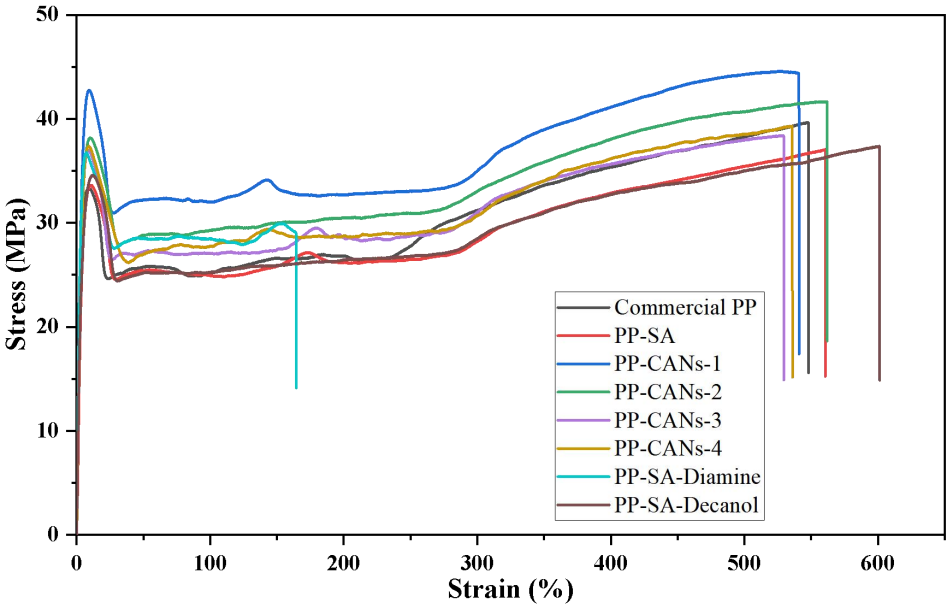

Fig. S18 Stress-strain data of PP-CANs and comparison samples

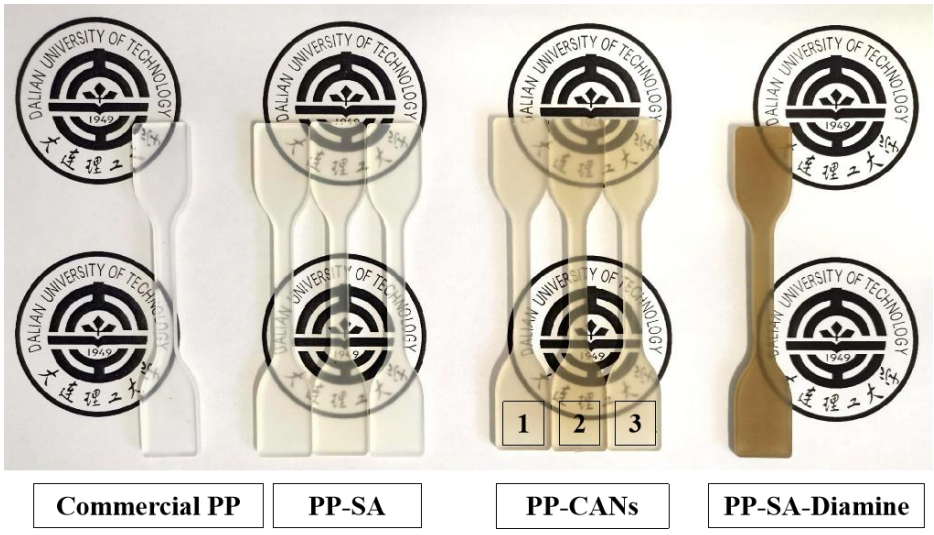

Fig. S19 Photographs of selected PP-CANs and comparison samples

Property data of recycled PP-CANs-3 samples

Table S3 Thermal properties of recycled PP-CANs-3 samples

Samples	T_c (℃)	T_m (℃)	χ_c (%)	$T_{d,5\%}$ (℃)
PP-CANs-3-r3[a]	126.0	164.6	49.0%	400.0
PP-CANs-3-r5[b]	126.9	164.5	47.1%	395.8

[a] PP-CANs-3 sample after 3 remodeling cycles.

[b] PP-CANs-3 sample after 5 remodeling cycles.

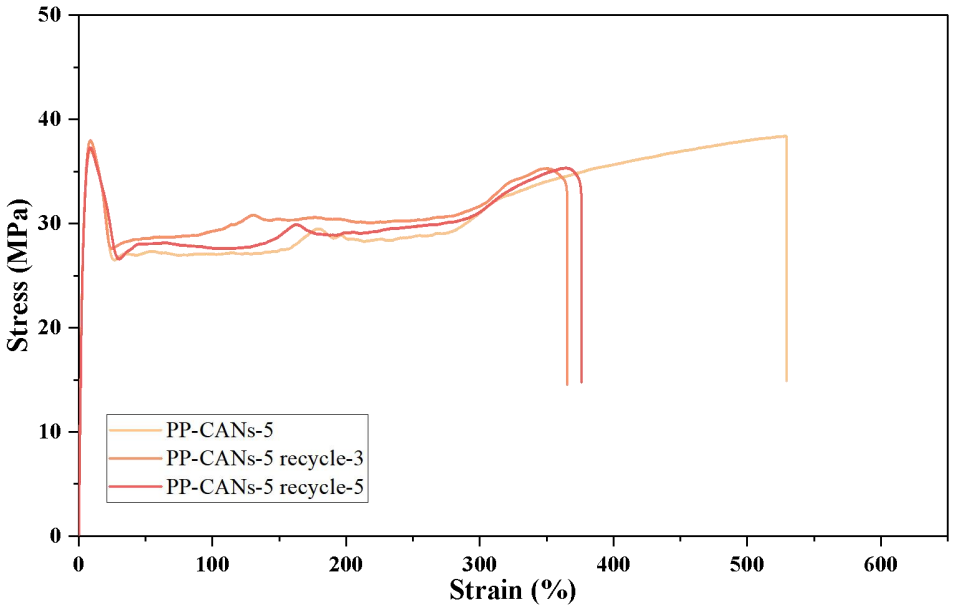

Fig. S20 Stress-strain data of recycled PP-CANs-3 samples

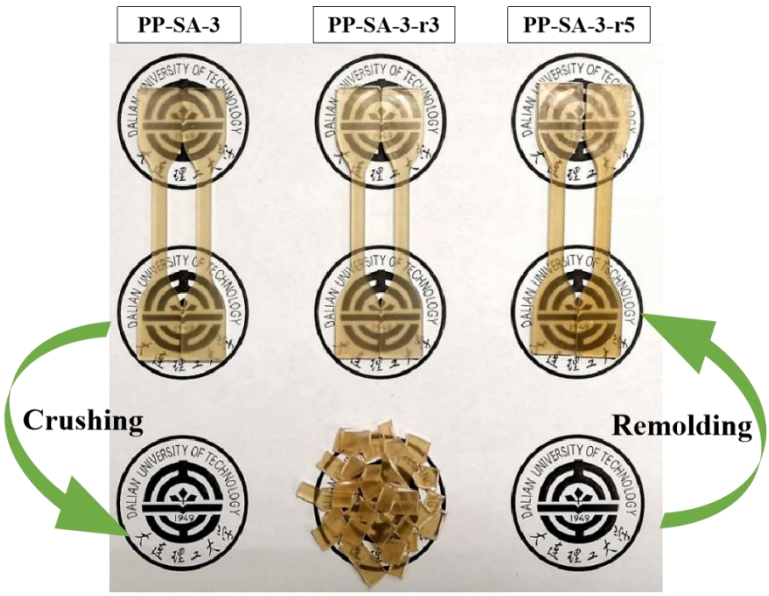

Fig. S21 Photographs of recycled PP-CANs-3 samples

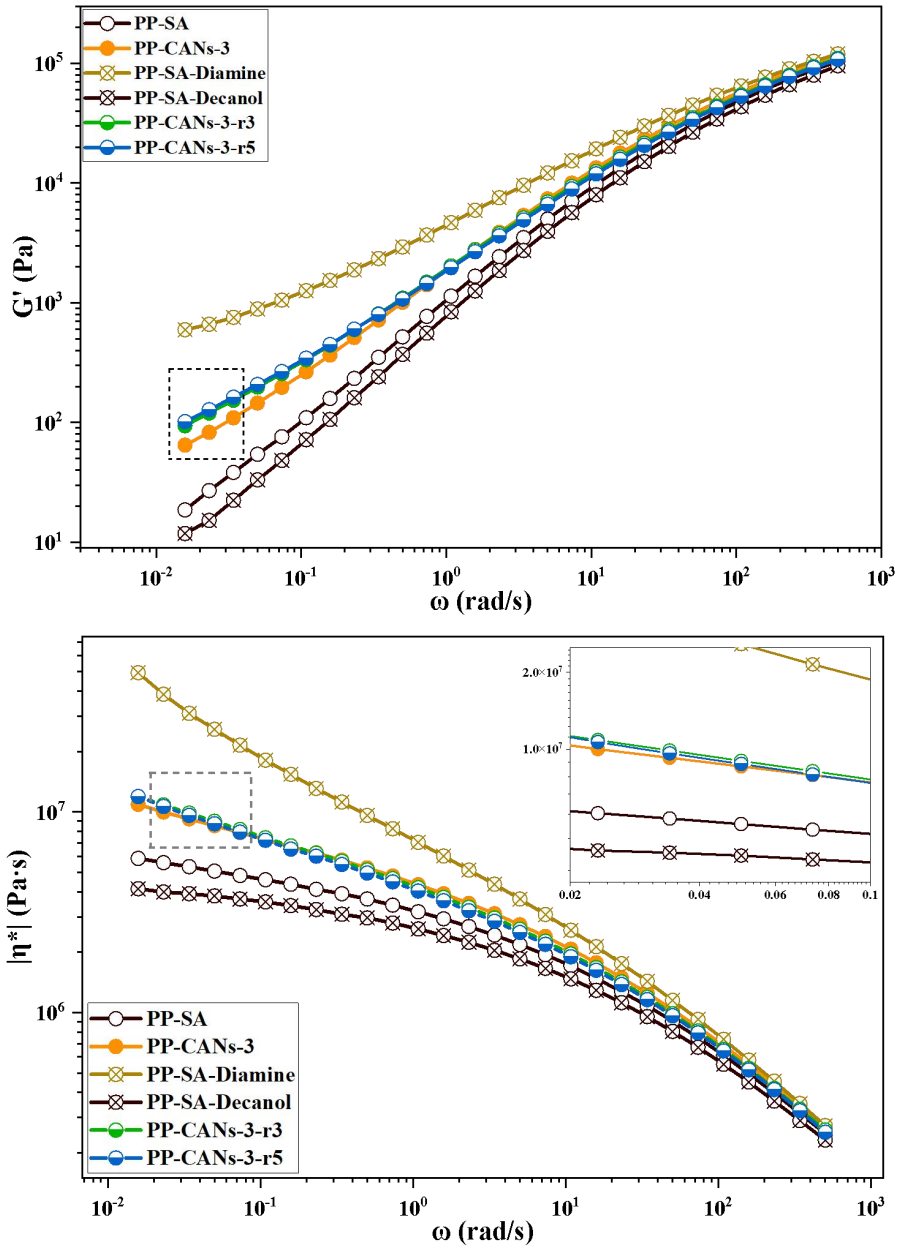

Fig. S22 Rheology curves of recycled PP-CANs-3 samples

Reference

[1] Mills E L, Ryan D G, Prag H A. et al. Itaconate is an anti-inflammatory metabolite that activates Nrf2 via alkylation of KEAP1. *Nature*, **2018**, 556(7699), 113-117.

[2] Bartoli G, Bosco M. Dalpozzo R, et al. $Zn(ClO_4)_2 \cdot 6H_2O$ as a Powerful Catalyst for a Practical Acylation of Alcohols with Acid Anhydrides. *European Journal of Organic Chemistry*, **2003**, 23, 4611-4617.

[3] Guo M, Zheng Y, Terell J. et al. Geminal dihalogen isosteric replacement in hydrated AI-2 affords potent quorum sensing modulators. *Chemical Communications*, **2015**, 51(13), 2617-2620.

[4] Delahaye M, Winne J M, Du Prez F E. Internal catalysis in covalent adaptable networks: phthalate monoester transesterification as a versatile dynamic crosslinking chemistry. *Journal of the American Chemical Society*, **2019**, 141, 15277-15287.

[5] Logan, S R, The kinetics of isotopic exchange reactions, *Journal of Chemical Education*, **1990**, 67, 371.

[6] Chung T C. Expanding Polyethylene and Polypropylene Applications to High-Energy Areas by Applying Polyolefin-Bonded Antioxidants. *Macromolecules*, **2019**, 52, 5618-5637.

[7] Moad G. The synthesis of polyolefin graft copolymers by reactive extrusion. *Progress in Polymer Science*,**1999**, 24, 81-142.

[8] Sclavons M, Franquinet P, Carlier V, et al. Quantification of the maleic anhydride grafted onto polypropylene by chemical and viscosimetric titrations, and FTIR spectroscopy. *Polymer*, **2000**, 41, 1989-1999.